Hydrogen ordering and magnetic transitions in $Y_yTb_{1-y}H(D)_x$ ($y=0.9$ and 0.2)

P. Vajda
Laboratoire des Solides Irradiés, CNRS, Ecole Polytechnique, F-91128 Palaiseau, France

O. J. Zogal
Institute of Low-Temperature and Structure Research, Polish Academy of Sciences, PL-50950 Wroclaw, Poland

(Received 21 July 1998; revised manuscript received 28 September 1998)

We have measured the electrical resistivity in the range 1.5–300 K of the hydrogenated alloy system $Y_yTb_{1-y}H(D)_x$, for $y=0.9$ and 0.2, and for hydrogen concentrations $0\leqslant x\leqslant 0.25$. It is found that, in the case $y=0.9$, hydrogen forms α^*-solid solutions up to concentrations $x_{\max}^{\alpha^*}=0.21(1)$. Like in binary α^*-YH_x, one observes ordering in the H sublattice near 170 K; a correlation between the periodicity of the helical antiferromagnetic (AF) structure in this alloy and that of the modulated chainlike H-H pair configuration in the ordered H sublattice is noted. For $y=0.2$, hydrogen precipitates at once as dihydride, which is, e.g., seen through the emergence of an H-dependent peak at 10 K due to the AF transition of β-TbH_2; the same is also noted, for $x>x_{\max}^{\alpha^*}$, in the case $y=0.9$. Hydrogen influences the various magnetic structures present by generally weakening the Ruderman-Kittel-Kasuya-Yosida polarization interaction. Thus, H addition results in a decrease of the spin-disorder scattering and of the magnetic manifestations at T_N^{Tb} and T_C^{Tb}. The low-T intrinsic resistivities are analyzed in terms of various types of spin-wave spectra for the two alloys and their interaction with hydrogen. [S0163-1829(99)10513-7]

I. INTRODUCTION

Rare-earth (R) metals absorb hydrogen readily, forming solid solutions (α phase) and hydrides (β and γ phases), depending on the concentration and the temperature range. Some of them, comprising the heavy lanthanides Ho, Er, Tm, and Lu as well as the assimilated Sc and Y, exhibit metastable solid solutions, α^* phase, which exist down to the lowest temperatures. Below a critical temperature $T_{cr}=150-170$ K, they arrange into quasilinear chainlike structures formed of H-H pairs located on second-neighbor tetrahedral sites along the c axis of the hcp unit cell. (Details of this phenomenon have been described, together with the general situation in the R-H systems, in a recent review by one of the present authors.[1])

One of the exciting aspects of the α^* phase is the possibility of observing the influence of hydrogen upon the magnetic order present at low temperatures in Ho, Er, and Tm and which has already revealed very characteristic effects related to the interaction of the anisotropic hydrogen configuration with the specific magnetic structures prevalent in each metal.[2,3] Now, as mentioned above, the ordering transition in the H sublattice occurs in the range 150–170 K, which lies in the paramagnetic region for the three metals in question. On the other hand, the metals Gd and Tb, with the respective ordering temperatures $T_N=293$ and 229 K,[4] do not form an α^* phase but precipitate at once into the dihydride β phase resulting in a two-phase ($\alpha+\beta$) region at these temperatures.

We were trying to circumvent this problem by choosing for our studies the alloy system Y_yTb_{1-y}, using the (nonmagnetic) yttrium component as hydrogen stock in the α^* phase and the terbium component as the magnetic counterpart for the interaction. The magnetic properties of Y-Tb alloys have been explored in detail by neutron diffraction[5-7] and magnetostriction.[8,9] Since, on the other hand, there exist extensive studies on the electronic and structural properties of the α^*-$YH(D)_x$ solid solutions,[1,10,11] this could give us a good starting point for the comprehension of the behavior of hydrogen in a Y-Tb alloy, which, to our knowledge, had not been attempted up to now. For the present resistivity experiment, which permits a very precise and detailed macroscopic exploration in view of a future neutron-diffraction study, we have selected Y_yTb_{1-y} alloys with two characteristic compositions: (a) $y=0.9$, with a $T_N\sim 50$ K (Ref. 5) but with sufficient Y to be able to test the H influence extrapolating from the Tb-free metal, $y=1$ (Ref. 12), and (b) $y=0.2$, with magnetic transitions at $T_N=196$ K and $T_C=99$ K (Ref. 5) and, hopefully, still enough Y to retain some hydrogen in solution. In addition, it seems that—apart from an early residual-resistivity study of very Y-rich Y-Tb alloys ($y=0.995$, 0.989, and 0.98) by Sugawara[13]—there exist no electrical measurements of this system, even without hydrogen.

In the following we will show that the H-solubility limit in the $Y_{0.9}Tb_{0.1}H_x$ alloy is about the same as for ''pure'' binary α^*-YH_x, while it is negligible in $Y_{0.2}Tb_{0.8}H_x$. We note an isotope effect on the H-sublattice ordering temperature and determine the H-migration energy through a quench experiment across the ordering range. In the $y=0.2$ sample, we observe a diminution and type change of spin-disorder scattering and a decrease of the T_N and T_C transitions with hydrogen; at the same time, we remark on the appearance of magnetic manifestations near 10 K due to the emerging dihydride (β-TbH_2) phase.

II. EXPERIMENTAL PROCEDURE

250-μm-thick Y_yTb_{1-y} alloy foils were purchased from the Ames Laboratory (Ames, IA) who prepared them by arc-melting nominally 4N material, with the following main me-

tallic impurities (in at. ppm): Y—27 Fe, 12 W, 7.5 Cu, 6 Ce, 3.7 Sc, 2.3 Tb, 1.5 Pr, 1.3 Cr; Tb—20 Fe, 14 W, 9 Y, 7.7 Ca, 5 Cu, 2.3 Cr, 1.5 Pb. They had been cold-rolled to their final thickness. 20×1 mm^2 specimens were cut from these foils and provided with four spot-welded Pt contacts for the electrical measurements. They were then annealed and degassed in a quartz furnace in a vacuum of $<10^{-6}$ Torr at 700–750 °C and subsequently loaded with hydrogen (or deuterium), homogenizing for 8 h at 500 °C (for details of the loading procedure, see, e.g., Ref. 1). The obtained concentrations were (to ±0.015) (a) $y=0.9$, $x=0$, 0.01, 0.05, 0.12, 0.15, 0.20, 0.22, 0.25H, and 0.1D; (b) $y=0.2$, $x=0$, 0.02, 0.06, 0.10, 0.15, 0.20H, and 0.1D. (As concerns the unloaded, $x=0$, specimens, we had measured their resistivities in both the as-delivered unannealed state and after a thermal treatment corresponding to the precharging conditions. Interestingly, the alloys with $y=0.9$ reacted to the anneal quite differently from those with $y=0.2$: while the latter had ''improved,'' in particular with regard to their magnetic manifestations, after elimination of the cold-roll effects, the former had increased in their residual resistivity due to the absorption of ~1 at. % H from the rest gas in the oven atmosphere, giving the $x=0.01$ specimen of the above series.)

Some of the specimens were submitted to a quenching treatment in order to check for possible effects of the disorder in the H sublattice. This was achieved by dipping the sample holder in liquid nitrogen before transfer towards the helium cryostat: the estimated cooling rate was of the order of 10^3 K/min as compared to the ordinary, slow, cooling rate of <0.5 K/min.

The electrical measurements were performed in a pumped liquid-helium cryostat between 1.5 and 300 K, using the classical four-point dc method and measuring up to seven specimens simultaneously (for details see, e.g., Ref. 2). The absolute precision of the resistivity data is several %, mainly due to uncertainties in the geometrical shape factor; the relative precision on a (ρ,T) couple is of the order of 10^{-4}, corresponding to $<10^{-8}\,\Omega$ cm in our experiment.

III. RESULTS

A. $y=0.9$

Figure 1 presents a series of typical specimens with various x concentrations, showing the global evolution through the whole measured temperature range 1.5–300 K. One notes a regular increase of the residual resistivity, $\rho_{\rm res}$, with x, resulting in a parallel shifted set of curves, up to a value of $x=0.20$; the next-higher presented concentration, $x=0.25$, exhibits a *lower* $\rho_{\rm res}$ value than $x=0.20$ and a low-T anomaly, indicating beginning precipitation of the (lower-resistivity) hydride phase. Let us also note here that the high-temperature slopes (taken between 250 and 300 K) show a slightly but definitely decreasing tendency with growing x, reaching a minimum for $x=0.22$, the next higher concentration $x=0.25$ possessing again higher slope, comparable to that of the $x=0.15$ specimen. Furthermore, one observes the anomaly near 170 K, growing with x and due to hydrogen sublattice ordering. Qualitatively, the above described phenomena are, until now, very similar to those observed on Tb-free $YH(D)_x$, and we shall analyze them in more detail below.

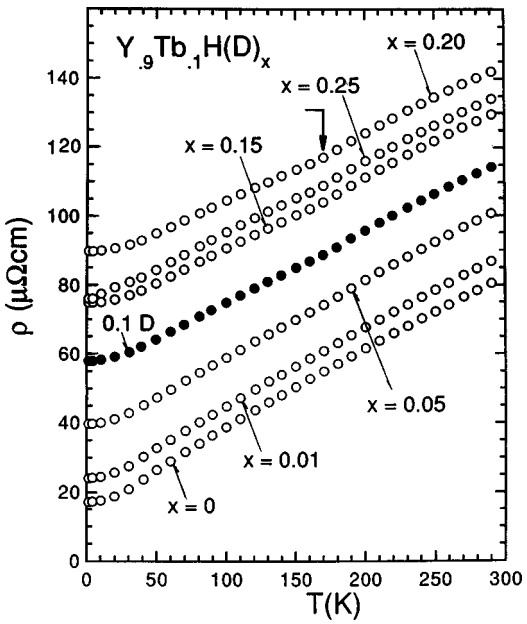

FIG. 1. Temperature dependence of the resistivity in the alloy system $Y_yTb_{1-y}H(D)_x$ for $y=0.9$ and various typical x values. The bold arrow indicates the ordering anomaly in the H sublattice at 170 K.

The plot in Fig. 2 shows the solubility limit of hydrogen in the α^* phase, given by the resistivity maxima in the exhibited isothermal $\rho(x)$ dependences, perusing all specimens: $x_{\rm max}(Y_{0.9}Tb_{0.1})=0.21(1)$ at. H(D)/unit, the same as for binary α^*-$YH(D)_x$, $x_{\rm max}=0.20(1)$, within measuring precision.[12] The slopes in the initial, linear, part of the curves give the specific resistivity increase per hydrogen atom [$\rho(0\ {\rm K})$ corresponds to $\rho_{\rm res}$]:

$$\Delta\rho/\Delta x\ \ (0\ \ {\rm K})=4.0(2)\ \ \mu\Omega\ {\rm cm/at.\ \%\ H(D)},$$

$$\Delta\rho/\Delta x\ \ (295\ \ {\rm K})=3.4(2)\ \ \mu\Omega\ {\rm cm/at.\ \%\ H(D)},$$

quite comparable to other similar α^*-$RH(D)_x$ systems.[1]

Figure 3 gives a collected view of the H-ordering region around 170 K, regrouping various specimens in order to emphasize various parameters, and shown in a differentiated plot, for more distinction. Thus we see clearly the presence of the anomaly in the $x=$ ''0.01'' specimen [Fig. 3(a)], con-

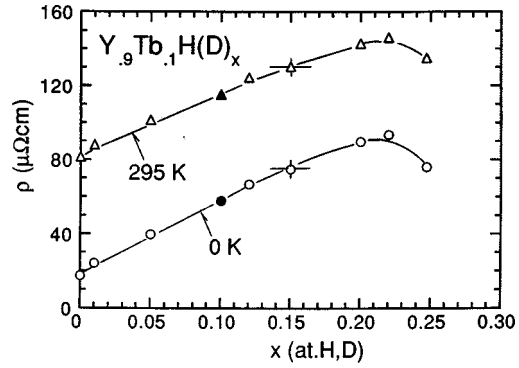

FIG. 2. Resistivity isothermals at room temperature and at 0 K (extrapolated), as a function of hydrogen concentration, for $y=0.9$, showing the solubility maximum near $x=0.21$.

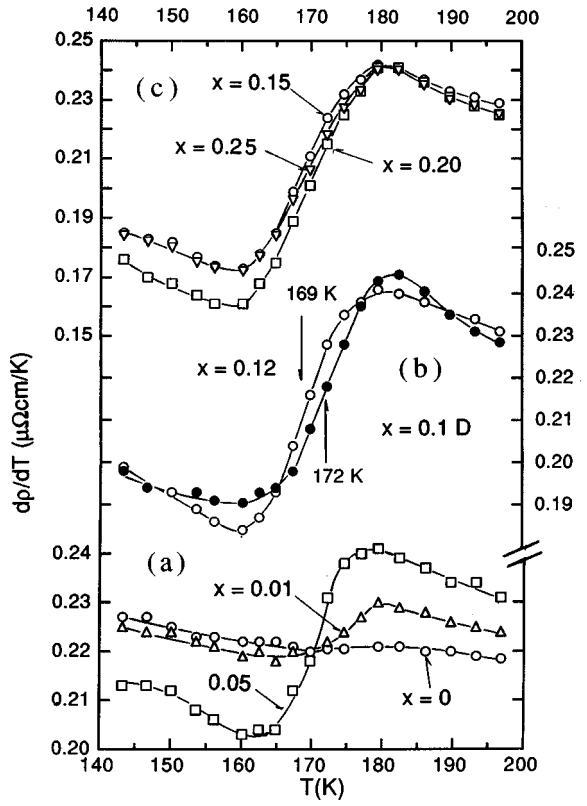

FIG. 3. Resistivity slopes in the $y=0.9$ alloy system around 170 K for various x concentrations. (a) $x=0$ (nonannealed), $x=''0.01''$ (annealed state, see text), and $x=0.05$; (b) isotope effect for $x=0.12$H and 0.1D; (c) $x=0.15$, 0.20, and 0.25 indicating a solubility maximum below $x=0.25$.

firming the classification established from its ρ_{res} value. On the other hand, its unannealed cold-rolled ''brother'' exhibits an anomaly in this interval which is at least an order of magnitude smaller, supporting its $x=0$ designation. Figure 3(b) exposes the isotope effect on the anomaly of two comparable x concentrations, $x=0.12$ H and 0.1D. The measured critical temperatures are

$$T_{\mathrm{cr}}(\mathrm{H})=169(1)\ \mathrm{K} \quad \text{and} \quad T_{\mathrm{cr}}(\mathrm{D})=172(1)\ \mathrm{K};$$

the anomaly temperatures are roughly the same as for pure binary α^*-YH(D)$_x$,[12] but the isotope effect is smaller in the present case, $\Delta T_{\mathrm{cr}}(\mathrm{D,H})=3(1)$ K, as compared to the 5(1) K of Ref. 12. Figure 3(c) shows the further growth of the anomaly amplitude with hydrogen concentration, reaching a maximum around $x=0.2$, the $x=0.25$ sample already possessing a smaller value. The anomaly amplitude, expressed as the difference between the maximum and the minimum values of $d\rho/dT$ around ~170 K, exhibits a maximum near $x=0.21$ and represents thus a satisfying analogy to the isotherms of Fig. 2.

It seemed interesting to see how the addition of Tb would influence the ordering capacity of the H sublattice, namely the migration energy of the H atoms after a quench across the ordering region. We have made this experiment on two concentrations, $x=0.22$ H and $x=0.1$ D, at the same time investigating an eventual isotope effect. The quench was very efficient, $\Delta\rho_q=2.5$–$3.5\,\mu\Omega$ cm, i.e., the quenched-in resistivity increase was about three times that in the pure

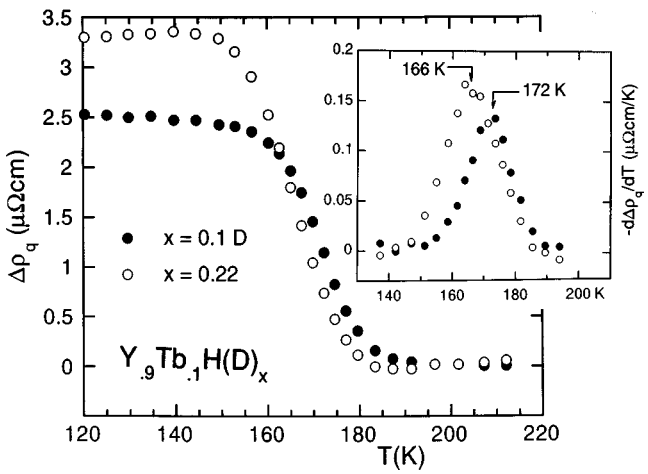

FIG. 4. Recovery curves of the quenched-in resistivity for $x=0.22$ and $x=0.1$D, in the $y=0.9$ system. The inset shows the slopes in the peak area used for the E_m determination (see text).

α^*-YH(D)$_x$ experiment,[12] due to the much higher cooling rates in our present, more performing, procedure, thus increasing the measuring precision in the subsequent annealing treatment. Figure 4 shows the recovery of the quenched-in $\Delta\rho_q$ for the two samples and the evolution of the slopes around the annealing stage in the inset. As for the binary α^*-RH(D)$_x$ systems,[1] the recovery process turns out a simple one-stage mechanism which can be analyzed by a first-order chemical-rate kinetics. As shown earlier,[14] the migration energy of the recovering species can be written as $E_m=k_B T_p^2[d\Delta\rho_q(T_p)/dT]/\Delta\rho_q(T_p)$, with the recovered resistivity fractions and corresponding slopes taken at the peak temperature, T_p. The measured annealing peaks are

$$T_p(\mathrm{H})=166(1)\ \mathrm{K} \quad \text{and} \quad T_p(\mathrm{D})=172(1)\ \mathrm{K},$$

some 3 K higher than the respective values in binary α^*-YH(D)$_x$ (Ref. 12). The resulting migration energies are also higher:

$$E_m^{\mathrm{Y_{0.9}Tb_{0.1}}}(\mathrm{H})=240(10)\ \mathrm{meV} \quad \text{and}$$

$$E_m^{\mathrm{Y_{0.9}Tb_{0.1}}}(\mathrm{D})=280(10)\ \mathrm{meV},$$

which is 30–40 meV more than for α^*-YH(D)$_x$, indicating a possible retarding effect of the Tb doping.

Let us now look for specific manifestations of the Tb presence, i.e., for any magnetic effects, for which Fig. 5 gives possible indications. Figure 5(a) is a differential plot of a series of concentrations in the low-T range and shows a peak at 43 K preceded by a minimum at 53 K, for the H-free specimen. This could be the Néel temperature given by Child *et al.*[5] as $T_{\mathrm{N}}\approx 50$ K for $y=0.9$ from their neutron-diffraction studies; the agreement is not too bad in view of the smallness of the observed magnetic intensities. The influence of hydrogen upon $T_{\mathrm{N}}^{\mathrm{Tb}}$ is immediate: the peak amplitude decreases strongly and is hardly visible for $x\geqslant 0.1$; the slopes also decrease—above but mainly below T_{N}—by a factor of 2 from $x=0$ to 0.20. The $T_{\mathrm{N}}^{\mathrm{Tb}}$ value itself shifts simultaneously to lower temperatures by about 10 K between $x=0$ and 0.05 (see also Table I).

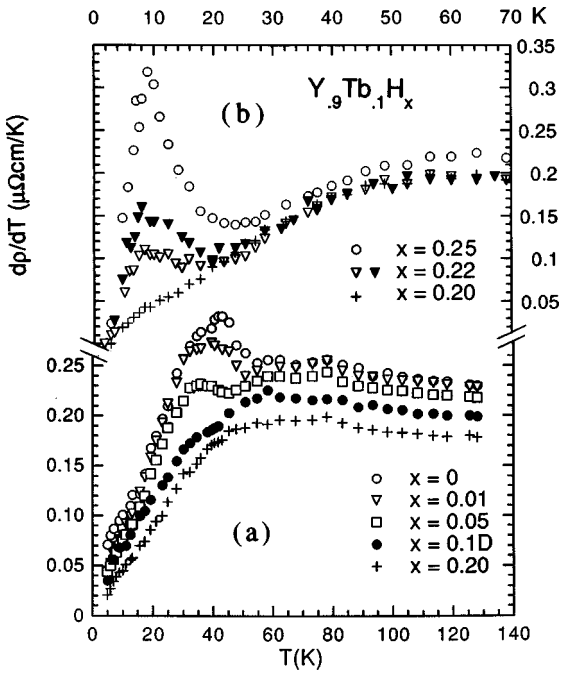

FIG. 5. Resistivity slopes in the $y=0.9$ alloy system for various x concentrations. (a) Around T_N^{Tb}; (b) around $T_N^{TbH_2}$; the $x=0.22$ sample is shown in the relaxed ($\triangledown$) and in the quenched state ($\blacktriangledown$).

A further increase in x, above the solubility limit $x_{max}^{\alpha *} \approx 0.2$, gives rise to a new phenomenon. Figure 5(b) shows the emergence of a new peak at $T=8-8.5$ K, for $x=0.22$, which grows strongly in amplitude and shifts somewhat to 9 K, for $x=0.25$. (Interestingly, a quench of the $x=0.22$ sample results in an increase of this anomaly.) In view of the absence of the peak for the specimens with $x \leqslant 0.20$, it seems justified to attribute it to the Néel temperature of the dihydride, β-TbH_2, which begins to precipitate out of the two-phase ($\alpha+\beta$) region for these concentrations. Its absolute value, however, is less than half of the ordering temperature of bulk β-TbH_2, $T_N^{TbH_2}=20-21$ K (Ref. 15).

B. $y=0.2$

A global view of the thermal resistivity evolution in the $y=0.2$ system (Fig. 6) looks quite different from that with $y=0.9$ (Fig. 1). Apart from the expected break near 200 K,

TABLE I. Magnetic transitions in the alloy $Y_{0.9}Tb_{0.1}H(D)_x$.

x	T_N^{Tb}/K[a]	$T_N^{TbH_2}$/K
0	53	
0.01[b]	50	
0.05	44	
0.1D	35	
0.12	33	
0.15	(32)	
0.20		
0.22		8–8.5
0.25		9.0

[a]Taken at the slope minimum.

[b]Corresponds to the heat-treated $x=0$ specimen.

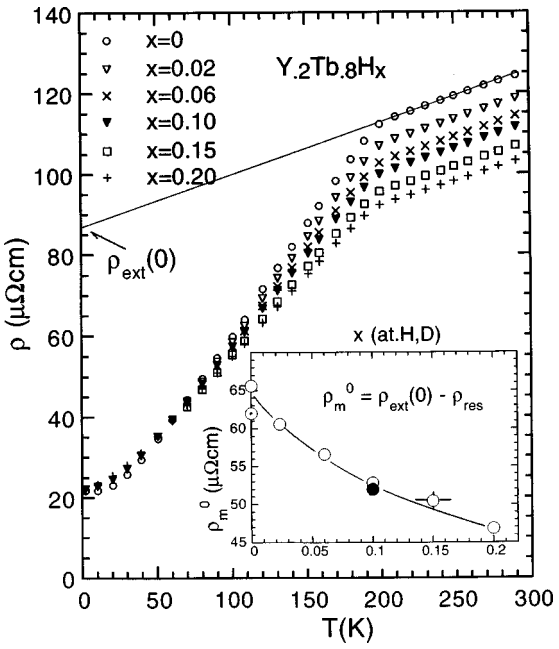

FIG. 6. Temperature dependence of the resistivity in the alloy system $Y_yTb_{1-y}H(D)_x$ for $y=0.2$ and various typical x values. The straight line shows the extrapolation of the high-T slope, in the case $x=0$, for the determination of the magnetic contribution ρ_m^0, shown in the inset as a function of x (the nonannealed $x=0$ sample is indicated by a central dot, the 0.1D sample in black).

which is the magnetic transition temperature determined by neutron diffraction and given as $T_N^{Tb}=196$ K for the H-free alloy,[5] one notes, with increasing x, a decreasing slope in the ordered range below T_N^{Tb}, but a practically unchanging residual resistivity, $\rho_{res}=21-22\ \mu\Omega$ cm for all x (see Table II for details). The slope decrease can be understood as a diminishing contribution of spin-disorder scattering to resistivity, ρ_m^0, determined after subtraction of the high-temperature phonon contribution extrapolated from the paramagnetic range to 0 K. The inset in Fig. 6 shows a regular decrease of ρ_m^0 with increasing x. (We have also plotted here the ρ_m^0 value of the unannealed $x=0$ specimen, for comparison.) Let us also mention the apparent decrease of the electron-phonon coupling, expressed by a slightly diminishing slope in the range above T_N^{Tb} with increasing x (Table II): it passes from $d\rho/dT(x=0)=0.128(3)$ to $d\rho/dT(x=0.20)=0.118(2)\ \mu\Omega$ cm/K, which is definitely more than the estimated 2% uncertainty.

A close look at the T_N^{Tb} area showed very little variation with x for the T_N^{Tb} value: a detailed determination through the second derivative yielded $T_N^{Tb}(x=0)=201.2$ K and $T_N^{Tb}(x=0.20)=200.0$ K, with a relatively regular interpolation for the intermediate x concentrations (Table II). This nearly H-independent T_N^{Tb} value is, together with the constant ρ_{res}, a first indication of negligible hydrogen solubility, i.e., practically no impurity scattering effect of the H atoms, but probably very early global interaction through hydride precipitation. The same conclusion can be drawn from the total absence of any sign for H-sublattice ordering in the usual range around 150–170 K.

Figure 7 is scanning the interval for ferromagnetic (FM) ordering around T_C^{Tb}. Child *et al.*[5] give from their neutron-

TABLE II. Specimen characteristics for the alloy $Y_{0.2}Tb_{0.8}H(D)_x$.

x	ρ_{res}[a] ($\mu\Omega$ cm)	$d\rho/dT$ (RT) ($\mu\Omega$ cm/K)	ρ_m^0 ($\mu\Omega$ cm)	$d\rho/dT$ (150 K)	T_N^{Tb}/K	T_C^{Tb}/K
0	21.75	0.128(2)	65.6	0.543	201.2	114.75
0[b]	22.2	0.125	62.0	0.531	200.7	
0.02	22.0	0.124	60.6	0.504	201.0	114.5
0.06	21.55	0.124	56.6	0.474	200.7	112.5
0.10	22.1	0.125	52.85	0.447	200.5	110.5
0.1D	21.35	0.123	52.0	0.440	200.5	112.0
0.15	20.8	0.122	50.45	0.423	200.2	112.5
0.20	21.85	0.118	46.85	0.394	200.0	112.5

[a]To $\pm 1\%$.
[b]Unannealed specimen.

scattering experiment a $T_C^{Tb}=99$ K for the $y=0.2$ alloy, while the x-ray lattice parameter measurements[8] and the magnetisation data of Ref. 9 give, for a composition close to ours, $y=0.165$, a $T_C^{Tb}=120$ K. The present resistivity measurements show a singularity at $T_C^{Tb}=115$ K for the H-free $x=0$ specimen, which flattens and broadens quickly upon hydrogenation. Its value decreases with increasing x, passing to $T_C^{Tb}(x=0.10)=110.5$ K, but stabilizes, for higher x, around 112–113 K (see Table II). (We wish to add here that no manifestation of T_C^{Tb} whatsoever could be seen on the unannealed cold-worked specimen.)

Furthermore, one notes (Fig. 8), at low temperatures, a superimposition of a new, hydrogen-dependent, resistivity contribution, best seen in differential form exhibited on the upper part of the figure. There, we observe a peak at 10 K, which appears for the lowest H concentration measured and whose amplitude keeps growing practically in a linear proportion with x. We attribute this peak tentatively to the magnetic transition of the dihydride β-TbH_2, $T_N^{TbH_2}=10.0(2)$ K. [The comparison with the $T_N^{TbH_2}$ manifestations in the $x>x_{max}^{\alpha *}$ specimens of the $y=0.9$ alloy (Fig. 5) is striking, even if, in the latter case, the $T_N^{TbH_2}$ was somewhat lower, 8–9 K, and, in addition, a quench effect was measured on the peak intensity, while no such phenomenon could be observed for $y=0.2$.]

Finally, no isotope effect was observed for the $x=0.1$D specimen through the whole measured temperature range, confirming, together with the absence of a quench effect, a negligible presence of hydrogen in solution capable of ordering into a sublattice.

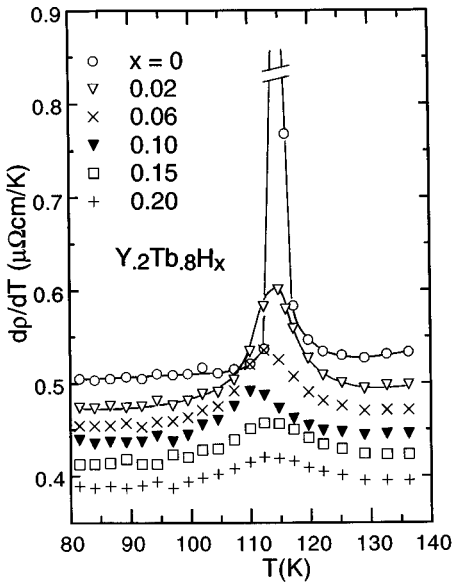

FIG. 7. Resistivity slopes in the $y=0.2$ alloy system around 115 K for various x concentrations, showing the singularity at T_C^{Tb} for $x=0$.

IV. DISCUSSION

The temperature dependence of the electrical resistivity in a magnetically ordering metal can be written as

$$\rho(T)=\rho_{res}+\rho_{mag}(T)+\rho_{ph}(T), \quad (1)$$

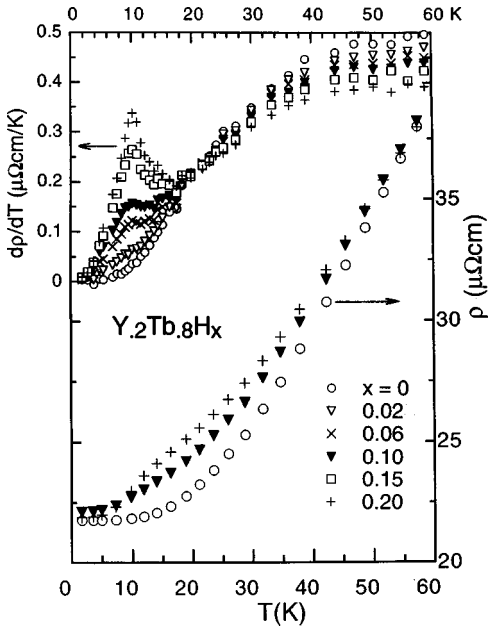

FIG. 8. Temperature dependence of the resistivity in the $y=0.2$ alloy system in the low-T region, for three selected x values; upper part: resistivity slopes around $T_N^{TbH_2}$ for all x.

where the last two terms are due to magnetic and to phonon excitations. It is, therefore, practical to analyze the influence of hydrogen upon each of the three above terms separately.

The magnetic structure of the whole range of Y_yTb_{1-y} alloys, $0 \leqslant y \leqslant 1$ (Ref. 5), with a more detailed analysis in the interval $0.93 \leqslant y \leqslant 0.98$ (Ref. 7), has been studied by neutron diffraction. It was found that the FM phase of Tb was rapidly destroyed upon dilution by Y, already for $y \geqslant 0.25$, while the AF helical ordering along the c axis of these hcp alloys, which is observed at least up to $y=0.98$, is stabilized resulting in an even stronger exchange interaction than in pure terbium.[6] Similar conclusions were drawn from recent ^{159}Tb-NMR experiments[16] on bulk and epitaxial Y-Tb alloys: yttrium is not to be considered a simple spin diluent but makes a substantial contribution to the transferred hyperfine field.

The interlayer turn angle in the helical structure increases, from $\sim 20°$ on, with increasing y and stabilizes, for $y \geqslant 0.6$, around 50°, corresponding to slightly more than seven planes per full spiral turn. It is interesting to recall, in this context, that the zigzagging H-H pair structure of the α^* phase observed by neutron scattering in the systems α^*-RD_x with $R=$ Sc, Y, and Lu (see, e.g., Ref. 1) and described in the Introduction is modulated with a wavelength of $3.75c$ between two configurational repetitions, corresponding to 7.5 interlayer planes. (Similar speculations had been undertaken by McKergow *et al.*[11] in the discussion of their original model of linear ordering of deuterium in yttrium but considering a modulation wavelength of $3c$ or six atomic layers.) On the other hand, another interesting point has been recently discussed by Andrianov,[17] who observed that the period of the helical magnetism in rare earths depended on their c/a ratio and, therefore, the turn angle could be modified by alloying or by applied pressure or simply by varying the temperature. A critical value of $(c/a)_{cr}=1.582(1)$ had been associated with an electronic topological transition related to the extreme diameter of the Fermi surface. We shall make use of these considerations in the discussion of the situation in the $Y_{0.9}Tb_{0.1}H_x$ system.

A. $y=0.9$

Even if the mechanism determining the hydrogen solubility in the α^* phase and, in particular, its limiting value $x_{\max}^{\alpha^*}$ is not quite clear yet—there is no obvious correlation between the measured $x_{\max}^{\alpha^*}$ and the atomic structural parameters of the rare earths in question, see, e.g., the discussion in Ref. 1—it seems reasonable to find the $x_{\max}^{\alpha^*}$ determined for the $Y_{0.9}Tb_{0.1}H_x$ system the same as in the binary α^*-$YH(D)_x$; note that a dilution of Y by 10 at.% Tb induces a relative change in the lattice parameters of less than 10^{-3} (Ref. 8). On the other hand, it might be worth mentioning that, in the Tb-free α^*-YH_x solutions, the c/a ratio is growing upon H addition and reaches a limiting value $c/a(x_{\max}^{\alpha^*})=1.582$ at room temperature, which is just the critical value associated with the electronic topological transition in Y quoted above.[17]

The evolution with hydrogen of the transition towards helical ordering at $T_N^{Tb} \sim 50$ K for $x=0$ [Fig. 5(a)] can be described through a decrease in the carrier concentration when adding hydrogen, which is the general case in R-H systems, where low-energy R-H bonding states are formed.[18] Pumping off electrons from the conduction band has immediate consequences upon all manifestations mediated by RKKY interactions, such as T_N^{Tb} and ρ_{mag} and also upon the electron-phonon interaction in the high-T slopes of the resistivities. Incidentally, it seems that the addition of hydrogen in solution has an analogous effect upon T_N^{Tb} as the dilution of Tb by Y. In fact, Rainford *et al.*[7] note a linear decrease of T_N^{Tb} in their Y_yTb_{1-y} alloys when going from $y=0.93$ to 0.98. When extrapolating to our case, $y=0.90$, adding $x=0.05$H results in a decrease of T_N^{Tb} by 9 K (Table I), which corresponds to the effect of a reduction by 1.5% Tb.

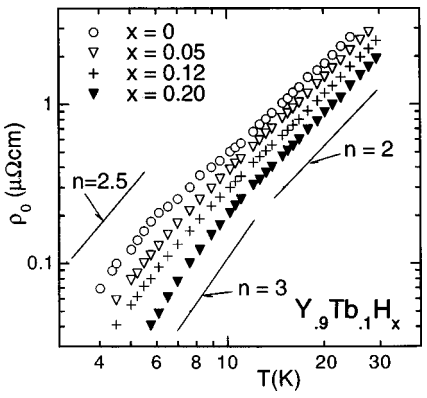

FIG. 9. Temperature dependence of the intrinsic resistivity in the low-T region for several concentrations in the $y=0.9$ alloy system, indicating the decomposition into two T^n dependences.

As to the magnetic contribution to the resistivity in Eq. (1), it can be investigated at low temperatures where the phonon part is negligible, after subtraction of ρ_{res}. We are showing such a dependence, for a selected number of specimens, in Fig. 9 in a double-logarithmic plot. Besides the general diminution of ρ_0 upon the addition of hydrogen, i.e., the suppression of ρ_{mag} with x, we note that the $\rho_0(T)$ dependences consist of two contributions: a low-T part proportional to T^n with n varying between 2.5 and 3, and, in the range $\sim$10–30 K, a perfect T^2 dependence. The latter is expected for helical antiferromagnetism,[4] while the former can be understood through a small anisotropy contribution of the crystal field, with a possible stiffening with x due to the presence of H-H pairs aligned along the c axis.

A final remark concerning the value of $T_N^{TbH_2}$ of the dihydride magnetism emerging for $x > x_{\max}^{\alpha^*}$ [Fig. 5(b)]. Bulk β-TbH_2 orders at 21 K in a sinusoidal incommensurate AF structure, with a propagation vector close to [116] which turns commensurate and parallel to [113] at 18 K, with a coexistence interval between the two configurations.[15] It is not clear, *a priori*, how the propagation vectors existing in the cubic (fcc) β phase will behave in an hcp environment with a smaller atomic volume, but a weakening of the exchange interaction leading to a decreasing $T_N^{TbH_2}$ seems not at all unreasonable.

B. $y=0.2$

The temperature-dependent spin-disorder resistivity can be written as[4]

$$\rho_m^0=(\hbar k_F/2\pi z)(m^*\Gamma/e\hbar^2)^2(g_J-1)^2J(J+1), \qquad (2)$$

where $(g_J-1)^2J(J+1)$ is the de Gennes factor, z the number of conduction electrons per atom, m^* their effective mass, k_F the Fermi wave vector, and Γ the exchange interaction parameter. Hence, its decrease with hydrogen (inset of Fig. 6) can be understood through a weakening Γ, caused by pumping off conduction electrons, probably a more efficient factor than the equally decreasing z in the denominator. Similar phenomena had already been reported before for polycrystalline α^*-ErH_x and α^*-TmH_x.[19]

As can be seen from Table II, the decrease with x of ρ_m^0 has a closely parallel variation to that of the slope in the AF-ordered interval between T_C^{Tb} and T_N^{Tb}, showing that the same mechanisms are acting both upon the T dependence of ρ_m (not too far below T_N^{Tb}) and upon its maximum value ρ_m^0. This means that the electron-phonon coupling in the ordered range is weakened in parallel with the exchange interaction, and this much more than the coupling above T_N^{Tb} (see Table II for the high-T slopes). On the other hand, the very slight (if any) decrease of T_N^{Tb} itself shows the little influence upon magnetic ordering that the hydrogen has in this Tb-rich system with strong anisotropy contributions.

At the same time, the hydrogen seems to have an immediate effect upon the FM transformation at T_C^{Tb} (see Fig. 7). In fact, T_C^{Tb} appears to be very sensitive to external influences such as alloying or metallurgical treatment. Thus, Child *et al.*[5] have shown that going from $y=0.1$ to 0.2 dropped T_C^{Tb} from 175 to 99 K, and for $y=0.25$ no T_C^{Tb} was detectable any longer. As already mentioned in Sec. III B, cold-rolling of the $x=0$ sample had completely suppressed the manifestation of T_C^{Tb}. Hence, the formation of cubic β-TbH_2 upon hydrogenation has a quite perturbing effect upon the c-axis ferromagnetism of this hcp alloy.

The emergence of the antiferromagnetism of β-TbH_2 at $T=10$ K (Fig. 8) perturbs also the spin-wave spectrum of the alloy at low temperature. Figure 10 presents a double-logarithmic plot of the intrinsic resistivity (practically just its magnetic contribution) as a function of temperature, showing a net T^4 dependence for the $x=0$ sample, while the H-loaded specimens exhibit rather a close to T^3 dependence. Now, the former corresponds[4] to spin-wave scattering in metals with conical magnetism, i.e., helical plus FM along the c axis, which is the case for pure $Y_{0.2}Tb_{0.8}$, while the latter represents rather the complex sinusoidal AF of the dihydride phase.[15] The fact that the absolute ρ_0 values *increase* as a function of x in this T range (while they had *decreased* in the $y=0.9$ system) is another sign of a superimposition of a new (β-TbH_2) magnetic contribution onto an old (Tb) existing one.

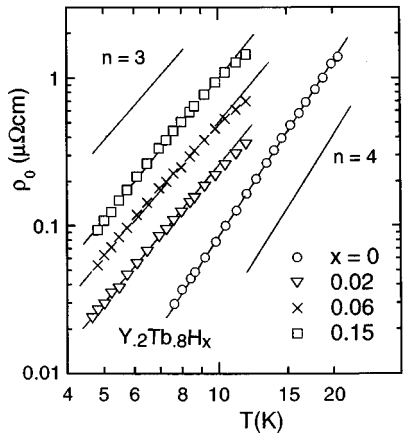

FIG. 10. Temperature dependence of the intrinsic resistivity in the low-T region for several concentrations in the $y=0.2$ alloy system, indicating the transition from a T^4 to a T^3 dependence upon hydrogenation.

V. CONCLUSIONS

The addition of hydrogen into the Y_yTb_{1-y} system leads to quite distinct behavior for the two alloys with $y=0.9$ and 0.2, respectively, mainly because the H atoms enter in solution (for $x\leqslant x_{max}^{\alpha^*}$) in the former case, while they precipitate at once as dihydride (β-TbH_2) in the latter. This leads, in addition to the appearance of (isotope-dependent) structural ordering in the H sublattice near 170 K, to the observation of the following phenomena due to the interaction of hydrogen with the different magnetic structures present: (i) decrease of ρ_{mag} with increasing x for both y values; (ii) strong decrease of T_N^{Tb} for $y=0.9$ and slight (if any) decrease for $y=0.2$; (iii) suppression and slight shift of T_C^{Tb} with x for $y=0.2$; (iv) emergence of $T_N^{TbH_2}$, for $x>x_{max}^{\alpha^*}=0.21(1)$, in the case $y=0.9$, and, for all $x>0$, in the case $y=0.2$; in both alloys is the value of $T_N^{TbH_2}\sim$const with x (8.5–10 K) but much smaller than in bulk β-TbH_2 (21 K).

Neutron-diffraction experiments are indicated and programmed for a qualitative understanding of the above described interaction of hydrogen with magnetism.

[1] P. Vajda, in *Hydrogen in Rare Earth Metals, Including RH_{2+x}-Phases*, Handbook on the Physics and Chemistry of Rare Earths, Vol. 20, edited by K. A. Gschneidner (North Holland, Amsterdam, 1995), p. 207.

[2] P. Vajda, J. N. Daou, J. P. Burger, C. Schmitzer, and G. Hilscher, J. Phys. F **17**, 2097 (1987).

[3] P. Vajda, J. N. Daou, J. P. Burger, G. Hilscher, and N. Pillmayr, J. Phys.: Condens. Matter **1**, 4099 (1989).

[4] B. Coqblin, *Electronic Structure of Rare Earth Metals and Alloys* (Academic, London, 1977).

[5] H. R. Child, W. C. Koehler, E. O. Wollan, and J. W. Cable, Phys. Rev. **138**, A1655 (1965).

[6] N. Wakabayashi and R. M. Nicklow, Phys. Rev. B **10**, 2049 (1974).

[7] B. D. Rainford, H. B. Stanley, and B. V. B. Sarkissian, Physica B & C **130**, 388 (1985).

[8] V. S. Belovol, V. A. Finkel, and V. E. Sivokon, Zh. Eksp. Teor. Fiz. **69**, 1734 (1975) [Sov. Phys. JETP **42**, 880 (1976)].
[9] S. A. Nikitin, A. S. Andreenko, V. P. Posyado, and G. E. Chuprikov, Fiz. Tverd. Tela (Leningrad) **19**, 1792 (1977) [Sov. Phys. Solid State **19**, 1045 (1977)].
[10] I. S. Anderson, J. J. Rush, T. J. Udovic, and J. M. Rowe, Phys. Rev. Lett. **57**, 2822 (1986).
[11] M. W. McKergow, D. K. Ross, J. E. Bonnet, I. S. Anderson, and O. Schaerpf, J. Phys. C **20**, 1909 (1987).
[12] P. Vajda, J. N. Daou, A. Lucasson, and J. P. Burger, J. Phys. F **17**, 1029 (1987).
[13] T. Sugawara, J. Phys. Soc. Jpn. **20**, 2252 (1965).
[14] J. N. Daou, P. Vajda, A. Lucasson, and J. P. Burger, Phys. Status Solidi A **95**, 543 (1986).
[15] P. Vajda, J. N. Daou, and J. P. Burger, Phys. Rev. B **36**, 8669 (1987); P. Vajda, J. N. Daou, and G. André, *ibid.* **48**, 6116 (1993).
[16] Y. Li, J. W. Ross, M. A. H. McCausland, D. S. P. Bunbury, M. R. Wells, and R. C. C. Ward, J. Phys.: Condens. Matter **8**, 11 291 (1996).
[17] A. V. Andrianov, J. Magn. Magn. Mater. **140-144**, 749 (1995); A. V. Andrianov and O. D. Chistiakov, Phys. Rev. B **55**, 14 107 (1997).
[18] A. C. Switendick, Solid State Commun. **8**, 1463 (1970); M. Gupta, *ibid.* **27**, 1355 (1978).
[19] J. N. Daou, P. Vajda, A. Lucasson, and P. Lucasson, Solid State Commun. **34**, 959 (1980); J. Phys. F **10**, L305 (1980).